0022-1554/86/$3.30
The Journal of Histochemistry and Cytochemistry

Vol. 34, No. 1, pp. 53-56, 1986
Printed in U.S.A.

Amphibian Limb Regeneration Curves Generated by the Scanning Laser Acoustic Microscope[1,2]

J.A. SLOBIN, D.L. STOCUM, and W.D. O'BRIEN, JR.[3]

Cell Biology Program (JAS), Department of Genetics and Development (DLS), and Bioacoustics Research Laboratory (WDO), University of Illinois, Urbana, IL 61801.

Received for publication August 21, 1985 and accepted for publication August 30, 1985 (5A0516P).

A scanning laser acoustic microscope was used to generate growth curves for amphibian limb regeneration. The mechanical properties of the specimen were converted into a visual image that was suitable for the measurements of limb growth. Bone, cartilage, muscle, dermis, and epidermis can be visualized.

KEY WORDS: Scanning laser acoustic microscope; Amphibian limb regeneration; Axolotl.

Introduction

The application of the scanning laser acoustic microscope, SLAM (Sonoscan, Inc., Bensenville, IL), in the area of biological research has been largely unexplored. Some applications include investigation of the fetal mouse heart (1), tendon fibers (2,3), mouse embryos (4), skin and wound tissue (5), and fatty livers (6). The generation of growth curves for amphibian limb regeneration presented another possible application because the curves could be generated from single individuals, eliminating several sources of error as well as the need to sacrifice large numbers of individuals. Since the SLAM translates the mechanical properties of the specimen into the visual image, the image of an axolotl (*Ambystoma mexicanum*) makes a fairly good "acoustic" subject.

Materials and Methods

The SLAM operates at an ultrasonic frequency of 100 MHz and has an approximate resolution in biological materials of 20 μm. The magnification (× 77) is sufficient to obtain accurately the data reported herein. However, the resolution and contrast of this particular SLAM are not sufficient to distinguish individual cells, although there are SLAMs that operate at higher frequencies and thus have better resolution. The specific distributions of ultrasonic propagation properties are found elsewhere (7-9).

Four axolotl larvae (age approximately 5 months, sex undetermined) were kept in 1% Holfreter's solution in glass bowls and fed every fourth day with a mixture of liver and Gainsburgers. Amputations were made on the right rear limb just distal to the knee under chlorotone anesthesia. Length of the stumps did not differ by more than 150 μm. The left leg was considered to be an internal control. Measurements were made at 24 ± 2 hr intervals for 25 days and at 48 ± 2 hr intervals through day 31. Both limbs were simultaneously examined optically and acoustically with the acoustic microscope. Data were retained by photographing the images on the monitors. Measurements for the growth curves were made directly from projections of the photographic slides or from composite photographs. Two axolotls were followed for the full 31 days and the other two died as a result of stress, most probably caused by handling or anesthesia.

Results and Discussion

The measurements that generated the graphs were taken from slides such as those reproduced in Figure 1. Blastema formation (Figures 1a-1d) and subsequent redifferentiation (Figures 1e-1i) are evident in both images (Figure 1) and graphs (Figures 2 and 3). Stages of dedifferentiation and regeneration are as suggested by Stocum (10). By day 1 after amputation (initial dedifferentiation) epidermis has migrated over the wound. By day 6 (early bud stage), the periosteal bone, cartilage, and muscle level to the amputation surface have dedifferentiated and the released blastema cells have formed an accumulation of cells, the blastema. The blastema grows through medium bud and late bud stages (days 7-9). At the late bud stage, it flattens distally into a paddle shape. By day 10 (early redifferentiation), a longitudinal groove becomes visible, marking the place where digits one and two will separate. By day 19 (early two-finger bud stage), the blastema is greatly increased in size. The shape of the blastema is somewhat angled relative to the position of the future knee joint. Cartilage condensation is visible but indistinct. On day 21 (late two-finger bud stage) the first two digits are elongating. New cartilage is somewhat more visible. By day 27 (third finger bud stage), digits one

[1] Supported in part by grants from the National Science Foundation (ENG 76-22450), the Campus Research Board of the University of Illinois at Urbana-Champaign, and the National Institutes of Health (RR07030).

[2] Presented in part at the symposium on the ADVANCES IN TECHNOLOGY, May 4, 1985, as part of the program at the annual meeting of the Histochemical Society, held in Crystal City, Virginia, May 3-5, 1985.

[3] Correspondence to: W.D. O'Brien, Jr., Bioacoustics Research Laboratory, Dept. of Electrical and Computer Engineering, University of Illinois, 1406 W. Green Street, Urbana, IL 61801.

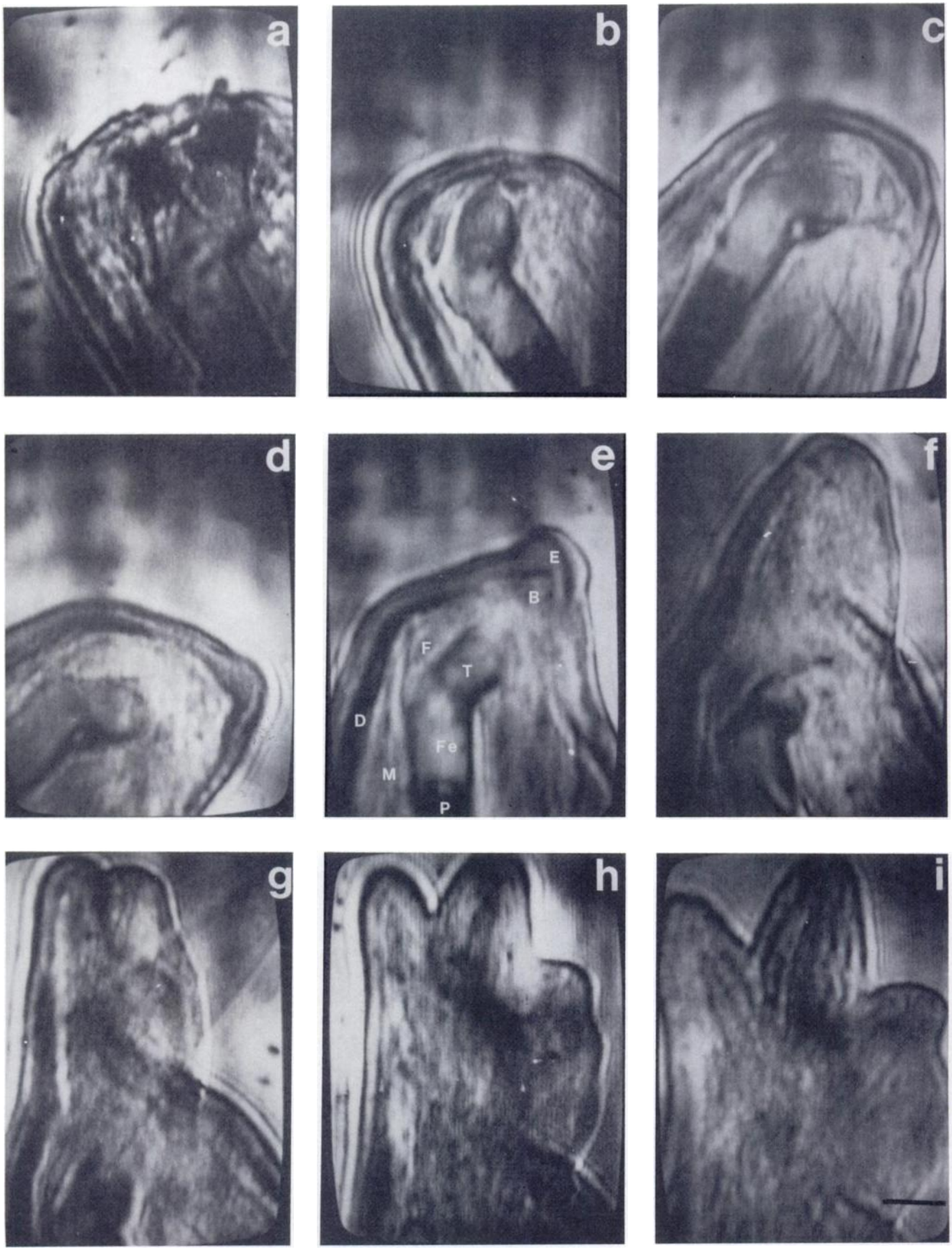
a
b
c
d
e
E
B
F
T
D
Fe
M
P
f
g
h
i

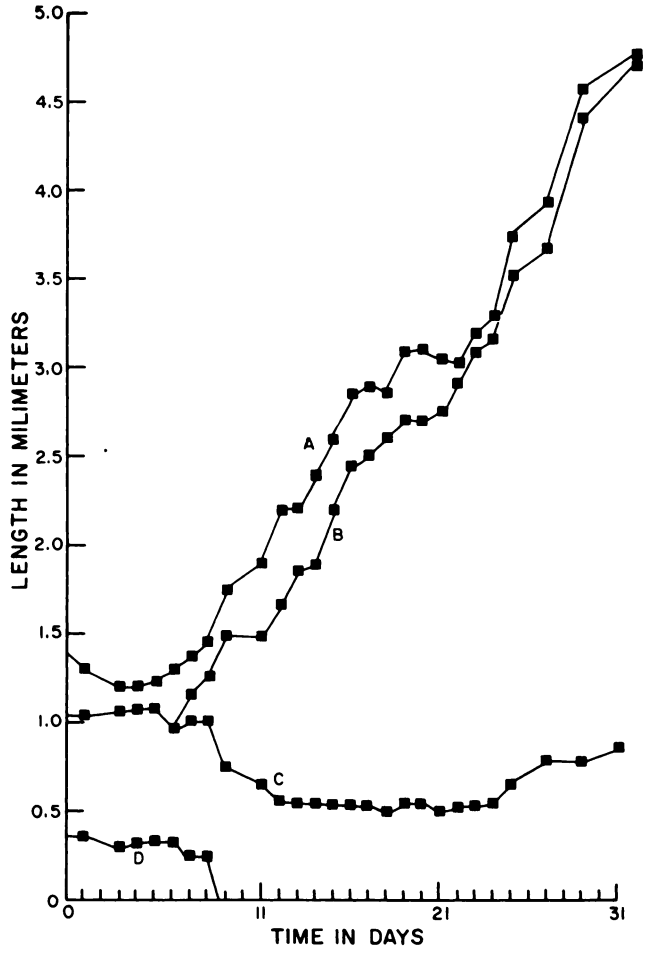

Figure 2. Bone regression and blastema formation for one axolotl (A-4). Measurements from acoustic micrographs were used to generate curves for bone regression and blastema formation of a single axolotl. A, total length of regenerate from knee joint to tip; B, length of regenerate from knee joint to epidermis; C, length of tibia; D, length of periosteal bone.

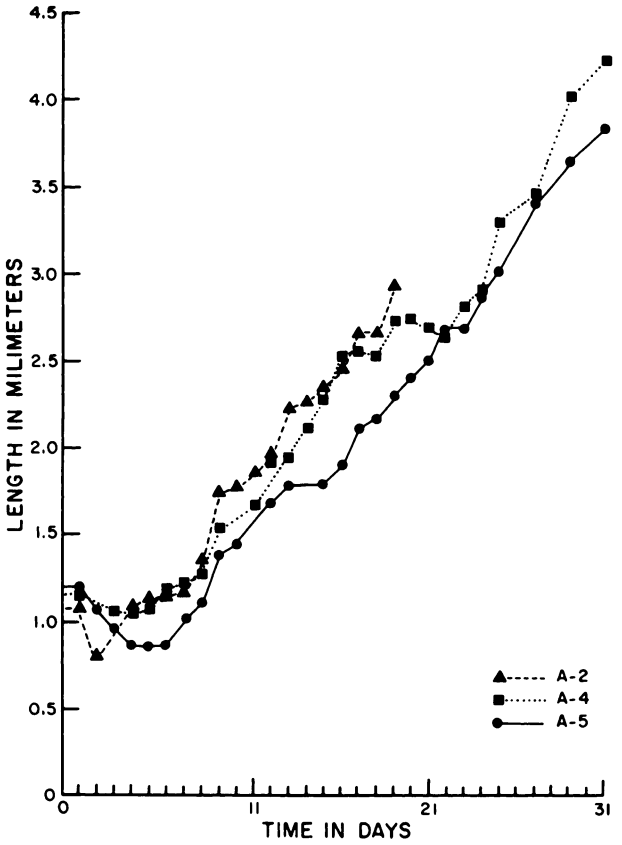

Figure 3. Normalized growth curves for three axolotls. Measurements from acoustic micrographs were used to generate curves showing limb regeneration for three axolotls (A-2, A-4, A-5).

and two are more distinct. The individual pieces of cartilage can be distinguished. Digit three is starting to elongate. By day 29, digit four is starting to separate. Redifferentiating cartilage is acoustically more distinct than the surrounding redifferentiating muscle cells.

Figure 2 shows curves plotted for overall growth of the blastema epidermal thickness, bone regressions, and subsequent cartilage recondensation of one axolotl. This is the first time such growth curves have been generated from a single axolotl. In more traditional studies, as many as 60 individuals may be sacrificed for a single curve. Data such as these can easily be normalized to eliminate differences resulting from unequal growth rates between individuals (Figure 3). Growth curves generated from the acoustic microscope images are similar in appearance to those generated from adult newt limbs by more traditional techniques (11), although our data show a somewhat quicker regeneration process (Figure 4). Larval forms of salamanders regenerate faster than adult forms. Also, our data were generated by amputation of the hindlimb, rather than the forelimb as in other studies.

Conclusion

The scanning laser acoustic microscope has many advantages over conventional techniques in the generation of growth curves. The use of the SLAM eliminates the need to sacrifice large numbers of individuals to generate a single curve. The traditional fixation and staining techniques are eliminated. Data are easily stored on slides.

Variations caused by differing levels of amputation and unequal rates of growth can be accounted for and, if necessary, normalized. Measurements can be kept very constant by the use of

Figure 1. Acoustic micrographs of the dedifferentiation and regeneration process of the same axolotl (*Ambystoma mexicanum*) limb. The time after amputation and stage are: (**a**) day 1, initial dedifferentiation; (**b**) day 6, early bud stage; (**c**) day 7, middle bud stage; (**d**) day 9, late bud stage; (**e**) day 10, early redifferentiation. Bone regression and blastema growth can be visualized at the site of amputation distal to the knee joint of an axolotl. P, periosteal bone; M, muscle; Fe, femur; D, dermis; T, tibia; F, fibula; B, blastema; E, epidermis; (**f**) day 19, early two-finger bud stage; (**g**) day 21, late two-finger bud stage; (**h**) day 27, third-finger bud stage; (**i**) day 29, fourth-finger bud stage. Bar = 0.4 mm.

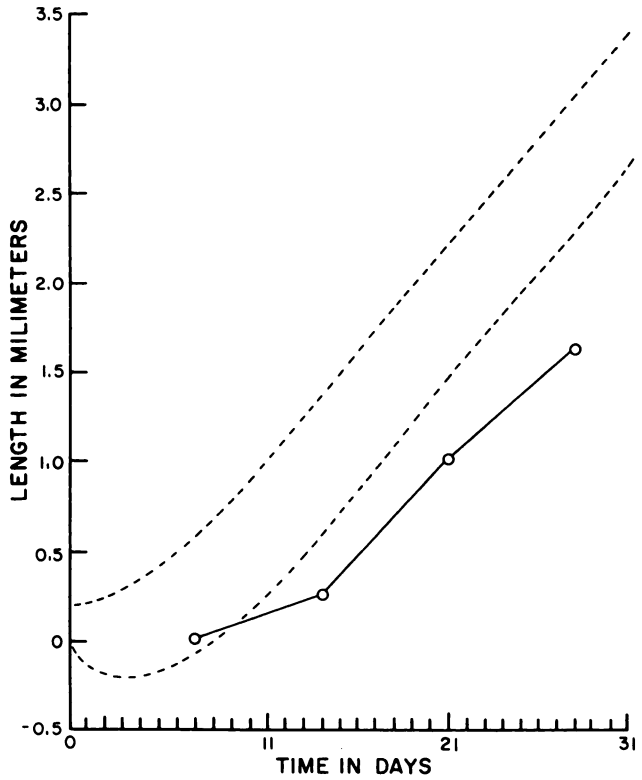

Figure 4. Acoustically generated data versus measurements by conventional methods. Growth curve measurements by conventional methods (11) (open circles) show a similar but not identical trend when compared to acoustically generated data. (Two dashed lines represent range of acoustically generated data.)

two internal controls. The unchanging diameter of the femur proximal to the knee joint over the period of study was a convenient marker when slides were enlarged for measurement.

The application of the SLAM to generate growth curves also allows for the effects of individual variation to be determined. Traditional techniques, which require many individuals to be sacrificed at a variety of times, show an average rather than a single and continuous process.

Literature Cited

1. Eggleton RC, Vinson FS: Heart model supported in organ culture and analyzed by acoustic microscopy. In Acoustical Holography, Vol. 7. Edited by LW Kessler. Plenum Press, New York, 1977, pp. 21–35
2. Goss SA, O'Brien WD Jr: Direct ultrasonic velocity measurements of mammalian collagen threads. J Acoust Soc Amer 65:507, 1979
3. Edwards CA, O'Brien WD Jr: Speed of sound in mammalian tendon threads using various reference media. IEEE Trans Sonics Ultrasonics SU-32:351, 1985
4. O'Brien WD Jr, Kessler LW: Examination of mouse embryological development with an acoustic microscope. Am Zool 15:807, 1975
5. O'Brien WD Jr, Olerud J, Reid JM, Shung KK: Quantitative acoustical assessment of wound maturation with acoustic microscopy. J Acoust Soc Amer 69:575, 1981
6. Tervola KMU, Grummer MA, Erdman JW, O'Brien WD Jr: Ultrasonic attenuation and velocity properties in rat liver as a function of fat concentration—a study at 100 MHz using a scanning laser acoustic microscope. J Acoust Soc Amer 77:307, 1985
7. Kessler LW, Yuhas DE: Acoustic microscope—1979. Proc IEEE 67:526, 1979
8. Embree PM, Tervola KMU, Foster SG, O'Brien WD Jr: Spatial distribution of the speed of sound in biological materials with the scanning laser acoustic microscope. IEEE Trans Sonics Ultrasonics SU-32:341, 1985
9. Tervola KMU, Foster SG, O'Brien WD Jr: Ultrasonics attenuation measurement techniques at 100 MHz with the scanning laser acoustic microscope. IEEE Trans Sonics Ultrasonics SU-32:259, 1985
10. Stocum DL: Stages of forelimb regeneration in *Ambystoma maculatum* and *Ambystoma tigrinum* after amputation through the wrist or upper arm. J Exp Zool 209:395, 1979
11. Iten LE, Bryant SV: Forelimb regeneration from different levels of amputation in the newt, Notophtalmus viridensen: length, rate and stages. Roux Arch 173:263, 1975